NUMERICAL METHODS FOR MULTISCALE ELLIPTIC PROBLEMS

PINGBING MING AND XINGYE YUE

Abstract. We present an overview of the recent development on numerical methods for elliptic problems with multiscale coefficients. We carry out a thorough study of two representative techniques: the heterogeneous multiscale method (HMM) and the multiscale finite element method (MsFEM). For problems with scale separation (but without specific assumptions on the particular form of the coefficients), analytical and numerical results show that HMM gives comparable accuracy as MsFEM, with much less cost. For problems without scale separation, our numerical results suggest that HMM performs at least as well as MsFEM, in terms of accuracy and cost, even though in this case both methods may fail to converge. Since the cost of MsFEM is comparable to that of solving the full fine scale problem, one might expect that it does not need scale separation and still retains some accuracy. We show that this is not the case. Specifically we give examples showing that if there exists an intermediate scale comparable to H, the size of the macroscale mesh, then MsFEM commits a finite error even with overlapping.

Contents

Date: September 22, 2003.

1991 *Mathematics Subject Classification.* 65N30, 74Q05, 74Q15, 74Q20, 39A12.

Key words and phrases. Heterogeneous Multiscale Method, Multiscale Finite Element Method, Scale Separation.

1. Introduction

In recent years the numerical computation of multiscale problems have emerged as an area of great promise. Among the most discussed examples is the elliptic problem with multiscale coefficients:

$$\begin{cases} -\operatorname{div}\Big(a^{\varepsilon}(\boldsymbol{x})\nabla u^{\varepsilon}(\boldsymbol{x})\Big) = f(\boldsymbol{x}) & \text{in } D, \\ u^{\varepsilon}(\boldsymbol{x}) = g(\boldsymbol{x}) & \text{on } \partial D, \end{cases} \tag{1.1}$$

where $\varepsilon \ll 1$ is a parameter that represents the ratio of the smallest and largest scales in the problem. This problem has attracted a great deal of attention because of its simplicity, its relevance to several important practical problems such as flow in porous media and mechanical properties of composite materials, and the extensive analytical work that has been done on it. Several different but related numerical techniques have been proposed, including wavelet homogenization techniques [19], solving analytical or effective homogenized equations [11, 18, 17, 38], finite element methods with multiscale test and trial functions [4, 6], multiscale finite element method [29, 30, 25], finite element method based on the *Residual-Free Bubble* methods (or the variational multiscale method) [13, 31, 40], and the heterogeneous multiscale method [21, 22, 23]. The purpose of the present paper is to give an overview of these methodologies as well as a thorough study of two representative techniques: The multiscale finite element method (MsFEM) and the heterogeneous multiscale method (HMM).

Before we discuss the more recent techniques, let us say a few words about some classical multiscale techniques that have been very successful for elliptic problems, e.g., the multi-grid method [12, 2, 36] and the fast multipole method [27]. Multi-grid method achieves optimal efficiency by relaxing the errors at different scales on different grids. It gives an accurate approximation to the detailed solutions of the fine scale problem (1.1). *In contrast, with the exception of MsFEM, the more* *recent activities center around designing multiscale methods with sublinear complexity* [23]*, i.e., the computational cost scales sublinearly with the cost of solving the fine scale problem as* $\varepsilon \to 0$*.* It is important to realize that our perspective has to be modified somewhat for this purpose. First we have to ask for less about the details of the solutions, since in many cases this would require us to solve the full fine scale problem and this already defeats our purpose. Secondly, we have to explore special features of the problem, such as self-similarity, periodicity and scale separation. This means that the method cannot be fully general but rather relies on special assumptions on the coefficients. Indeed if $a^\varepsilon(\boldsymbol{x})$ does not have any special features, (1.1) is just as hard as a general elliptic problem:

$$\begin{cases} -\operatorname{div}\Big(a(\boldsymbol{x})\nabla u(\boldsymbol{x})\Big) = f(\boldsymbol{x}) & \text{in } D, \\ u(\boldsymbol{x}) = g(\boldsymbol{x}) & \text{on } \partial D, \end{cases} \tag{1.2}$$

and we cannot hope for a method with sublinear cost. On the other hand, it is undesirable for the numerical methods to be too small a range of applicability. Therefore a balance has to be reached between specificity and generality. One common feature found in many practical problems is separation of scales. Indeed it has been the designing principle of many modern multiscale methods such as HMM to be able to take full advantage of the possible scale separation in the problem, while in the absence of scale separation, the method is similar to the fine scale solvers.

One exception is MsFEM. For problems of the type (1.1), MsFEM incurs a cost that is comparable to that of a fine scale solver, even for problems with scale separation. For this reason, one might expect that MsFEM might still retain some accuracy even for problems without scale separation, as in the case of fine scale solvers. We will show that this is not the case. *Specifically we will give explicit examples showing that MsFEM converges to the wrong solution if there is an intermediate scale which is comparable to the size of the macroscale mesh.*

There are many important problems without separation of scales. In the absence of a better understanding at the present time the choice for such problems seems to be either the full fine scale solvers or resorting to ad hoc procedures such as turbulence models. Other special features have to be identified in order to construct sublinear algorithms that do not resort to uncontrolled approximations.

This paper is organized as follows. In the following section we will give an overview of the different multiscale methods. Sections 3 and 4 are devoted to a thorough study of HMM and MsFEM. We pick these two methods since they represent two somewhat opposite philosophies. Section 3 is devoted to problems with scale separation. This is the case when both methods have been thoroughly analyzed. Here we compare the cost and accuracy of HMM and MsFEM for several classes of problems. We will show that MsFEM incurs an $\mathcal{O}(1)$ error if the specific details of the fine scale properties are not explicitly used. In Section 4 we consider problems without scale separation. In this case both methods may fail to converge but we show that in terms of numbers, the quality of the HMM result is at least comparable to that of MsFEM. Finally we draw some conclusions in Section 5.

2. An overview of multiscale methods

To present the methods, we consider the typical multiscale problem

$$\begin{cases} -\operatorname{div}\Big(a^{\varepsilon}(\boldsymbol{x})\nabla u^{\varepsilon}(\boldsymbol{x})\Big) = f(\boldsymbol{x}) & \text{in } D, \\ u^{\varepsilon}(\boldsymbol{x}) = 0, & \text{on } \partial D \end{cases} \tag{2.1}$$

where $a^{\varepsilon}(\boldsymbol{x}) = \Big(a^{\varepsilon}_{ij}(\boldsymbol{x})\Big)$ is assumed to be a symmetric matrix satisfying

$$\lambda|\xi|^2 \le \sum_{i,j=1}^{2} a^{\varepsilon}_{ij}\xi_i\xi_j \le \Lambda|\xi|^2, \quad \forall \xi \in \mathbb{R}^2,$$

with $0 < \lambda \le \Lambda$.

We will use standard notations for Sobolev spaces $W^{k,p}(D)$ [1] for $k > 0$ and $p > 1$, which are denoted by $H^k(D)$ while $p = 2$.

2.1. General methodologies.

2.1.1. *Generalized finite element method.* Generalized finite element method [7, 6] is a finite element method on a macroscopic mesh with modified basis functions that are obtained by solving (1.1) with $f = 0$ and nodal boundary conditions. This method is a perfect strategy for one dimensional problems. It was extended to high dimensions in [29]. Other methods for modifying the basis functions are found in [13, 31].

2.1.2. *Wavelet homogenization.* The main idea is to derive numerically effective operators at the macroscale scale by successively eliminating the small scales. The most natural framework for carrying this out is to represent the numerical solutions in wavelet basis [19]. Even though after eliminating the smaller scales, the effective operator becomes dense, Engquist and Runborg [26] have shown that they can be very well approximated by sparse operators.

2.1.3. *Model refinement.* One of the most important issues in solving problems of the type (1.1) is to recover the details of ∇u^{ε} since they contain information of great practical interest, such as the stress distribution in a composite material or velocity field in a porous medium. Oden and co-workers [38] proposed the idea of local model refinement for this purpose. After the homogenized equation is solved, the original fine scale problem is solved locally around places where derivative information is required, with the homogenized solution as the Dirichlet boundary condition. Denote by Ω the domain in which the microscale information of u^ε is needed. Consider the following auxiliary problem:

$$\begin{cases} -\operatorname{div}\Big(a^{\varepsilon}(\boldsymbol{x})\nabla \overline{u}^{\,\varepsilon}(\boldsymbol{x})\Big) = f(\boldsymbol{x}), & \boldsymbol{x}\in\Omega_\eta, \\ \overline{u}^{\,\varepsilon}(\boldsymbol{x}) = U_H(\boldsymbol{x}), & \boldsymbol{x}\in\partial\Omega_\eta, \end{cases} \tag{2.2}$$

where Ω_η satisfies $\Omega\subset\Omega_\eta\subset D$ and $\operatorname{dist}(\partial\Omega,\partial\Omega_\eta)=\eta$. We then have

$$\Big(\frac{1}{|\Omega|}\int_\Omega |\nabla(u^\varepsilon-\overline{u}^{\,\varepsilon})|^2\,dx\Big)^{1/2} \le \frac{C}{\eta}\Big(\|U_0-U_H\|_{L^\infty(\Omega_\eta)}+\|u^\varepsilon-U_0\|_{L^\infty(\Omega_\eta)}\Big). \tag{2.3}$$

Here U_H and U_0 are respectively the numerical and analytical solutions to the homogenized problem.

2.1.4. *Heterogeneous multiscale method.* There are two main components in the heterogeneous multiscale method: An overall macroscopic scheme for the macroscale variables on a macroscale grid and estimating the missing macroscopic data from the microscopic model. For (1.1), the macroscopic solver can be chosen simply as the standard piecewise linear finite element method over a macroscopic triangulation $\mathcal{T}_H$ of mesh size H. The data that need to be estimated is the stiffness matrix. This is equivalent to evaluating the effective quadratic form $A(V,V)$ for $V\in X_H$, where X_H is the macroscopic finite element space. If we had an explicit expression for $A(V,V)$, such as

$$A(V,V)=\int_D\sum_{i,j=1}^{2}A_{ij}(\boldsymbol{x})\frac{\partial V}{\partial x_i}\frac{\partial V}{\partial x_j}\,dx, \tag{2.4}$$

we can then evaluate the integral by numerical quadrature. In the absence of an explicit representation such as (2.4), we need to estimate the value of the integrand in (2.4) at quadrature points. This is done as follows.

Let $\boldsymbol{x}_K$ be the barycenter of the element $K\in\mathcal{T}_H$, and let $I_\delta=\boldsymbol{x}_K+\delta I$, where $I=[0,1]^d$ (see the let one in Figure 2). δ is chosen such that a^ε restricted to I_δ gives an accurate enough representation of the local variations of a^ε. For $V\in X_H$, let $\mathcal{R}(V)$ be the solution of

$$\operatorname{div}\Big(a^{\varepsilon}(\boldsymbol{x})\nabla\mathcal{R}(V)\Big)=0, \qquad \boldsymbol{x}\in I_\delta, \tag{2.5}$$

with the boundary condition that $\mathcal{R}(V)-V$ is periodic with period δI.

We then approximate the integrand of (2.4) at $\boldsymbol{x}_K$ by

$$\sum_{i,j=1}^{2}A_{ij}(\boldsymbol{x}_K)\frac{\partial V}{\partial x_i}\frac{\partial V}{\partial x_j}\approx\frac{1}{|I_\delta|}\int_{I_\delta}\sum_{i,j=1}^{2}a_{ij}^{\varepsilon}(\boldsymbol{x})\frac{\partial}{\partial x_i}\mathcal{R}(V)\frac{\partial}{\partial x_j}\mathcal{R}(V)\,dx. \tag{2.6}$$

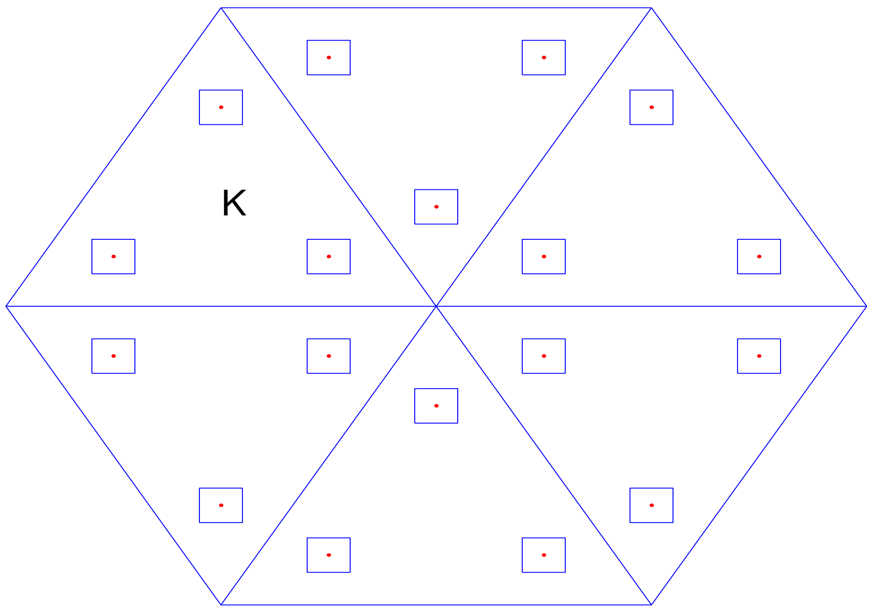

FIGURE 1. Illustration of HMM for solving (1.1). The dots are the quadrature points. The little squares are the microcell $I_\delta(x_\ell)$.

The approximating bilinear form A_H is defined as

$$A_H(V,W) := \sum_{K\in\mathcal{T}_H} \frac{|K|}{|I_\delta|}\int_{I_\delta}\sum_{i,j=1}^{d} a_{ij}^{\varepsilon}(\boldsymbol{x})\frac{\partial}{\partial x_i}\mathcal{R}(V)\frac{\partial}{\partial x_j}\mathcal{R}(W)\,dx,$$

for any $V,W\in X_H$. The HMM solution $U_H\in X_H$ is defined by

$$A_H(U_H,V)=(f,V)\qquad\forall V\in X_H. \tag{2.7}$$

HMM can be naturally extended to higher order by using higher order finite elements as the macroscopic solver (see [24]). In this case, a cell problem has to be solved at each quadrature point, and the higher-order numerical quadrature schemes has to be employed to approximate the bilinear form. HMM can also be extended to the case when the isoparametric finite elements are exploited as the macroscopic solver.

So far the formulation of HMM is completely general. The main point, however, is that HMM offers substantially savings of cost (compared to solve the full fine scale problems) for problems with scale separation. This is done by appropriately choosing δ. If the problem happens to be locally periodic, we may choose I_δ to be the local period. However, it is important to emphasize that it is not necessary for the coefficient $a^\varepsilon(\boldsymbol{x})$ to have the form $a(\boldsymbol{x},\boldsymbol{x}/\varepsilon)$ in order to have such savings, so long as there is scale separation. Without scale separation or any other special features of the problem, HMM simply degenerates to a fine scale solver.

In many cases, we would like to have accurate information on ∇u^ε. From U_H, one can construct an approximation $\overline{u}^\varepsilon$ to u^ε. A general strategy for constructing $\overline{u}^\varepsilon$ is to use the method of local corrections, as done by Oden et al [38] (see also (2.2) and (2.3)). For the special case of periodic homogenization problems, with $\delta = \varepsilon$, one may simply define on each element K,

$$\overline{u}^\varepsilon = U_H + \Big(\mathcal{R}(U_H) - U_H\Big)_p,$$

here $(f)_p$ means the periodic extension of f outside I_δ.

Even though the method is quite general, the analysis of HMM has so far only been carried out for the case when $a^\varepsilon(\boldsymbol{x}) = a(\boldsymbol{x}, \boldsymbol{x}/\varepsilon)$. First we discuss the case when $a(\boldsymbol{x}, \boldsymbol{y})$ is periodic in $\boldsymbol{y}$, say with period $I = [0,1]^d$.

Theorem 2.1. [24, Theorem 1.1, Theorem 1.2] *Let u^ε, U_0 and U_H be the solution of* (1.1)*, the homogenized equation and* (2.7)*, respectively. If $a(\boldsymbol{x}, \boldsymbol{y})$ is periodic in $\boldsymbol{y}$ with period I, then there exists a constant C such that*

$$\|U_0 - U_H\|_{H^1(D)} \le C\Big(H + \nu_0(\varepsilon, \delta)\Big). \tag{2.8}$$

$$\|U_0 - U_H\|_{L^2(D)} \le C\Big(H^2 + \nu_0(\varepsilon, \delta)\Big). \tag{2.9}$$

$$\|U_0 - U_H\|_{L^\infty(D)} \le C\Big(H^2 + \nu_0(\varepsilon, \delta)\Big)|\ln H|. \tag{2.10}$$

Let $\overline{u}^\varepsilon$ be the reconstructed microstructure as above, we have

$$\Big(\sum_{K \in \mathcal{T}_H} \|\nabla(u^\varepsilon - \overline{u}^\varepsilon)\|^2_{L^2(K)}\Big)^{1/2} \le C\Big(\sqrt{\varepsilon} + H + \nu_0(\varepsilon, \delta)\Big), \tag{2.11}$$

In general,

$$\nu_0(\varepsilon, \delta) \le C\Big(\frac{\varepsilon}{\delta} + \delta\Big).$$

But if $\delta = \mathbb{N}\varepsilon$ and $\mathbb{N}$ is an integer, then

$$\nu_0(\varepsilon, \delta) \le C\delta.$$

In view of (2.9) and (2.10) and the classic estimates for u^ε [5, 10, 46]

$$\|u^\varepsilon - U_0\|_{L^2(D)} \le C\varepsilon, \qquad \|u^\varepsilon - U_0\|_{L^\infty(D)} \le C\varepsilon,$$

an application of the triangle inequality gives

$$\|u^\varepsilon - U_H\|_{L^2(D)} \le C\Big(\varepsilon + H^2 + \nu_0(\varepsilon, \delta)\Big). \tag{2.12}$$

$$\|u^\varepsilon - U_H\|_{L^\infty(D)} \le C\Big(\varepsilon + H^2 + \nu_0(\varepsilon, \delta)\Big)|\ln H|. \tag{2.13}$$

Many practical problems are better modelled by an a^ε which is a locally stationary random field. We refer to [24] for the precise setting. In this case, we have

Theorem 2.2. [24, Theorem 1.2] *For the case when $a(\boldsymbol{x},\boldsymbol{y})$ is stationary random field, under the conditions of* [24, Theorem 1.1]*, we have*

$$\mathbb{E}\|U_0-U_H\|_{H^1(D)}\le C\Big(H+\nu_0(\varepsilon,\delta)\Big),$$

where

$$\nu_0(\varepsilon,\delta)\le\begin{cases}C\Big(\dfrac{\varepsilon}{\delta}\Big)^{\kappa} & d=3\\ \textit{remains open} & d=2\\ C\Big(\dfrac{\varepsilon}{\delta}\Big)^{1/2} & d=1\end{cases}$$

with

$$\kappa=\frac{6-12\gamma}{25-8\gamma}\qquad 0<\gamma<\frac12.$$

The conditions in [24, Theorem 1.2] are mainly strong mixing, uniform ellipticity and some regularity on $a(\boldsymbol{x},\boldsymbol{y})$.

2.1.5. *Multiscale finite element method.* We discuss the over-sampling MsFEM([29, 25]) which reduces the effect of the boundary layers occurring at the inter-element boundaries. MsFEM is an extension of an old idea of Babuska [7], which incorporates the fine scale information into the basis functions by solving the original fine scale differential equations on each element with proper boundary conditions.

For any $K\in\mathcal{T}_H$ with nodes $\{x_i^K\}_{i=1}^3$, let H_K denote the size of K, $P_1(K)$ the set of linear polynomials defined in K, and $\{\varphi_i^K\}_{i=1}^3$ the basis of $P_1(K)$ satisfying $\varphi_i^K(x_j^K)=\delta_{ij}, i,j=1,2,3$. For any $K\in\mathcal{T}_H$, we denote by $S=S(K)$ (see Figure 2) a macro-element which contains K and satisfies the following conditions: $H_S\le C_1H_K$ and $\operatorname{dist}(\partial K,\partial S)\ge\delta_0H_K$ for some positive constants C_1, δ_0 independent of H.

Let $MS(S)$ be the multiscale finite element space spanned by $\psi_i^S, i=1,2,3$, with $\psi_i^S\in H^1(S)$ being the solution of the problem

$$-\operatorname{div}\Big(a^{\varepsilon}(x)\nabla\psi_i^S\Big)=0\quad\text{in } S,\quad \psi_i^S|_{\partial S}=\varphi_i^S. \tag{2.14}$$

Here $\{\varphi_i^S\}_{i=1}^3$ is the nodal basis of $P_1(S)$ such that $\varphi_i^S(x_j^S)=\delta_{ij}$, $i,j=1,2,3$. The over-sampling multiscale finite element base functions over K are defined by

$$\bar\psi_i^K=c_{ij}^K\psi_j^S|_K\quad\text{in } K,$$

with the constants c_{ij}^K so chosen that

$$\varphi_i^K=c_{ij}^K\varphi_j^S|_K\quad\text{in } K.$$

The existence of the constants c_{ij}^K is guaranteed because $\{\varphi_j^S\}_{j=1}^3$ also forms the basis of $P_1(K)$.

Let $\mathcal{M}(K)=\operatorname{span}\{\bar\psi_i^K\}_{i=1}^3$ and $\varPi_K:\mathcal{M}(K)\to P_1(K)$ the projection

$$\varPi_K\psi=c_i\varphi_i^K\quad\text{if } \psi=c_i\bar\psi_i^K\in\mathcal{M}(K).$$

Let $\overline{V}_H$ be the finite element space

$$\overline{V}_H = \{ \psi_H \mid \psi_{H|_K} \in \mathcal{M}(K), \ \forall K \in \mathcal{T}_H \},$$

and define $\varPi_H : \overline{V}_H \to \varPi_{K\in\mathcal{T}_H} P_1(K)$ through the relation $\varPi_H \psi_{H|_K} = \varPi_K \psi_H$ for any $K \in \mathcal{T}_H$, $\psi_H \in \overline{V}_H$. The over-sampling multiscale finite element space is then defined as

$$V_H = \{\psi_H \in \overline{V}_H \mid \varPi_H \psi_H \in X_H \subset H_0^1(D)\}.$$

The over-sampling MsFEM is: Find $U_H \in V_H$ such that

$$\sum_{K\in\mathcal{T}_H} \int_K a^\varepsilon(\boldsymbol{x}) \nabla U_H \nabla V \, dx = (f, V), \quad \forall V \in V_H. \tag{2.15}$$

The analysis of MsFEM has only been carried out for the case when $a^\varepsilon(\boldsymbol{x}) = a(\boldsymbol{x}/\varepsilon)$ and $a(\boldsymbol{y})$ is periodic in $\boldsymbol{y}$, in this case, we have

Theorem 2.3. [30, 25] *Let u^ε and U_H be the solutions of* (2.1) *and* (2.15)*, respectively. If $a(\boldsymbol{y})$ is periodic with period I, then there exists a constant C which is independent of ε, δ and H such that*

$$\Big(\sum_{K\in\mathcal{T}_H} \|\nabla(u^\varepsilon - U_H)\|^2_{L^2(K)} \Big)^{1/2} \le C \Big(\sqrt{\varepsilon} + H + \frac{\varepsilon}{H} \Big), \tag{2.16}$$

and

$$\|u^\varepsilon - U_H\|_{L^2(D)} \le C \Big(H^2 + \frac{\varepsilon}{H} \Big). \tag{2.17}$$

The above error bounds may be extended to the locally periodic coefficients, i.e., $a^\varepsilon(\boldsymbol{x}) = a(\boldsymbol{x}, \boldsymbol{x}/\varepsilon)$ with $a(\cdot, \boldsymbol{y})$ is periodic in $\boldsymbol{y}$ by combining the techniques in [14] and [30, 25, 45]. However, the accuracy in L^2 norm may deteriorate if the algorithm is not adopted to the new feature of the coefficients.

If $a^\varepsilon(\boldsymbol{x}) = a(\boldsymbol{x}/\varepsilon)$ with $a(\boldsymbol{y})$ is periodic, then (2.12) and (2.13) can be improved to

$$\|u^\varepsilon - U_H\|_{L^2(D)} \le C \Big(H^2 + \frac{\varepsilon}{\delta} \Big),$$
$$\|u^\varepsilon - U_H\|_{L^\infty(D)} \le C \Big(H^2 + \frac{\varepsilon}{\delta} \Big) |\ln H|.$$

Compared the above two and (2.11) with Theorem 2.3, we may conclude that the accuracy of HMM and MsFEM is comparable in this special case since we always assume that δ is commensurable with H. Moreover, once we know the exact period of a^ε, we only need to solve the cell problem over I_ε, in this case, the consistency error term ε/δ vanishes, HMM get better results.

2.2. **Special technique for the periodic homogenization problem.** Next, we discuss methods that are more specific. Such methods rely on a specific form of the coefficient $a^\varepsilon(\boldsymbol{x}) = a(\boldsymbol{x}, \boldsymbol{x}/\varepsilon)$ where the function $a(\boldsymbol{x}, \boldsymbol{y})$ is periodic in $\boldsymbol{y}$ with some period, say I.

2.2.1. *Solving homogenized equations.* Since there exists a very well-developed homogenization theory, one may use these theory for numerical purposes. This is done in [11, 4, 18, 17] for example. The leading order term in u^ε is obtained by solving the homogenized equation:

$$\begin{cases} -\operatorname{div}\Big(A(\boldsymbol{x})\nabla U(\boldsymbol{x})\Big) = f(\boldsymbol{x}) & \text{in } D, \\ U(\boldsymbol{x}) = g(\boldsymbol{x}) & \text{on } \partial D. \end{cases} \tag{2.18}$$

To obtain finite ε correction and to recover the microstructural behavior of u^ε, one needs to solve further the corrector problem: find $u_1(\boldsymbol{x}, \boldsymbol{x}/\varepsilon)$ such that

$$\begin{cases} -\operatorname{div}\Big(a^\varepsilon(\boldsymbol{x})\nabla u_1\Big(\boldsymbol{x}, \dfrac{\boldsymbol{x}}{\varepsilon}\Big)\Big) = \operatorname{div}\Big(a^\varepsilon(\boldsymbol{x})\nabla U_0(\boldsymbol{x})\Big) & \text{in } D, \\ u_1(\boldsymbol{x}, \boldsymbol{y}) \qquad \text{is periodic in } \boldsymbol{y}. \end{cases}$$

A subtle issue in this approach is the presence of boundary layers [9]:

$$\|u^\varepsilon(\boldsymbol{x}) - \Big(U_0(\boldsymbol{x}) + u_1\Big(\boldsymbol{x}, \frac{\boldsymbol{x}}{\varepsilon}\Big)\Big)\|_{H^1(D)} \le C\sqrt{\varepsilon}.$$

2.2.2. *Two-scale finite element methods.* The main idea is to use multiscale test and trial functions of the form $\varphi(\boldsymbol{x}, \boldsymbol{x}/\varepsilon)$ to probe simultaneously the macro and microscale behavior of the solution u^ε. The two-scale finite element space X_H is the traces of the two-scale spaces $\mathcal{S}^p(\mathcal{T}_H; \mathcal{S}^\mu_{\text{per}}(\mathcal{T}_h))$,

$$X_H = \mathcal{R}^\varepsilon \mathcal{S}^p(\mathcal{T}_H; \mathcal{S}^\mu_{\text{per}}(\mathcal{T}_h)) \qquad \text{with} \qquad (\mathcal{R}^\varepsilon V)(x) = V(x, y)_{|_{y=\frac{x}{\varepsilon}}}.$$

Here the macroscopic finite element space $\mathcal{S}^p$ consists of piecewise polynomials of degree p over $\mathcal{T}_H$; and the finite element space over the cell εI, say $\mathcal{S}^\mu_{\text{per}}$, which consists of periodic piecewise polynomials of degree μ over the microscopic mesh $\mathcal{T}_h$. This idea has been used in the analytical work of Allaire [3], E [20] and Nguesteng [37], among others. The work of Schwab et al [34, 41, 42] develop this into a numerical tool. The following result on the accuracy of this method is proved in [35]. Denote by u^ε_H the two-scale finite element solution. If H is an integer multiple of ε, then

$$\begin{aligned} \|u^\varepsilon - u^\varepsilon_H\|_{H^1(D)} \le\, & C_1(k) H^{\min(p,k)} \Phi_n(p,k) \|f\|_{H^k(D)} \\ & + C_2(s) h^{\min(\mu,s)} \Phi_n(\mu,s) \|f\|_{H^{\mu+s}(D)}. \end{aligned} \tag{2.19}$$

Here $\Phi_n(p,k) \le Cp^{-(k-n+1)}$ and $\Phi_n(\mu,s) \le C\mu^{-(s-n+1)}$.

3. Problems with scale separation

3.1. **Computational cost.** To compare the cost we make the assumption that the total cost is proportional to the total degrees of the freedom used in the algorithm. This is reasonable since we typically use multi-grid method as the fine scale solver.

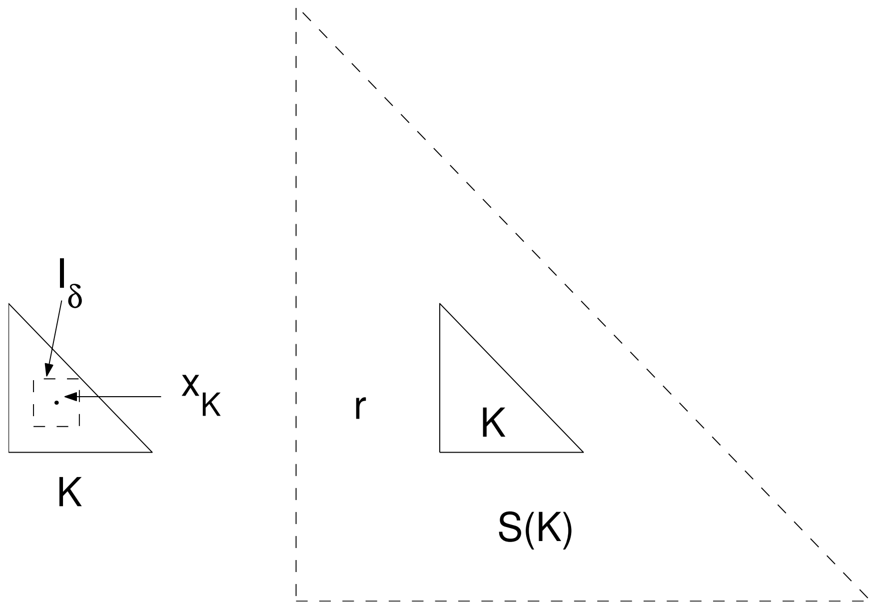

FIGURE 2. Computational cell used for solving fine scale problem in HMM and MsFEM. The element K is depicted in solid line. The computational cell I_δ for HMM and $S(K)$ for MsFEM are depicted in dashed line.

Given parameters ε, H and δ, assuming that M points per wavelength (which is $\mathcal{O}(\varepsilon)$) are used, then the total cost for the full fine scale solver is

$$COST(\text{fine scale solver}) = M^d \varepsilon^{-d}.$$

Assuming that the size of the overlap in MsFEM is r, then the total cost for MsFEM is

$$COST(\text{MsFEM}) = (1+3r)^d M^d \varepsilon^{-d}.$$

The ratio between the two is

$$\frac{COST(\text{fine scale solver})}{COST(\text{MsFEM})} = \frac{1}{(1+3r/H)^d} < 1,$$

i.e., MsFEM is in general more expensive than the full fine scale solver. This is consistent with our numerical results on standard PC; The fine scale solver on a 1024×1024 grid takes about 1 minute. MsFEM on the same fine grid takes more than 10 minutes if we set $r = H$.

The cost for HMM is:

$$COST(\text{HMM}) = M^d H^{-d} \Big(\frac{\delta}{\varepsilon}\Big)^d.$$

Hence the ratio between the cost of HMM and the cost of MsFEM is

$$\frac{COST(\text{HMM})}{COST(\text{MsFEM})} = \Big(\frac{\delta}{H}\Big)^d \frac{1}{(1+3r/H)^d}.$$

The ratio between the cost of HMM and the cost of the direct fine scale solver is

$$\frac{COST(\text{HMM})}{COST(\text{fine scale solver})} = \Big(\frac{\delta}{H}\Big)^d.$$

As long as we can take $\delta < H + 3r$, HMM incurs a smaller cost than the full fine scale solver.

The parameters δ and H are determined by the tolerance factor, denoted by TOL. For MsFEM, the accuracy cannot be better than $\sqrt{\varepsilon}$ (see the error estimates in Theorem 2.3), so to make a meaningful comparison, we have to take

$$TOL > \mathcal{O}(\sqrt{\varepsilon}).$$

Considering the case when $\nu_0(\varepsilon/\delta) = \mathcal{O}(\varepsilon/\delta)$ (this is expected to be true even for random problems above two dimension). For the HMM solution to have an error less than the tolerance TOL, we need to have $H = \mathcal{O}(TOL)$ and $\delta = \varepsilon/TOL$. Hence

$$\frac{\delta}{H} = \mathcal{O}\Big(\frac{\varepsilon}{(TOL)^2}\Big) < 1.$$

i.e., HMM always saves in this case.

HMM may incur an additional cost in order to recover locally the fine scale information. This is problem-dependent.

The above discussion is for general problems with scale separation. For the special case of periodic homogenization problems, we can take $\delta = \varepsilon$ for HMM, and modify MsFEM so that the solutions to the corrector problem can be used in constructing the basis function [28]. This is both an advantage and disadvantage for MsFEM. It is an advantage since computational cost can be greatly reduced if $\varepsilon \ll 1$. It is an disadvantage since this is very special and the original method has to be drastically changed to adopt to this special case. In any case, there does not seem to be such cost-saving modification for more general problems with scale separation. For this reason, we will disregard this special change in the following discussion.

Some problems require solving (1.1) repeatedly with different right-hand side. Both HMM and MsFEM can take advantage of the fact that in this case the macroscale stiffness matrix can be computed for once and used repeatedly. This might be a potential source of savings of cost for problems such as the multi-phase porous medium flows. If there is a time scale separation in the problem, for example if the change of saturation field behind the oil/water front is much slower than the change of the front itself, then it might be possible to update the entries in the macroscale stiffness matrix (required for solving the pressure equation) for elements away from the front rather infrequently and still maintain reasonable accuracy. Unfortunately such time scale separation does not seem to be present in these problems. In addition to this, there is the issue of how the saturation equation is solved. The work of [28] simply solves the full fine scale problem.

Compared with the full fine scale solutions, both HMM and MsFEM have the advantage that they are easy to be parallelized. It has been suggested that MsFEM saves in memory compared with direct fine scale solvers. This is only true if the microscale information is not required, or if it is recovered through a post-processing step as discussed for HMM. Otherwise the complete set of basis functions in MsFEM have to be stored for retrieving such information, leaving us with no savings in memory.

3.2. **Numerical examples for two-scale problems.** We will start with an example of the simplest two-scale problem, the periodic homogenization problem.

$$\begin{cases} -\operatorname{div}\Big(a\Big(\boldsymbol{x},\dfrac{\boldsymbol{x}}{\varepsilon}\Big)\nabla u^\varepsilon(\boldsymbol{x})\Big) = f, & \text{in} \quad D, \\ u^\varepsilon(\boldsymbol{x}) = 0, & \text{on} \quad \partial D, \end{cases} \tag{3.1}$$

where $f = 10$, and the coefficients $a^\varepsilon(\boldsymbol{x}, \boldsymbol{x}/\varepsilon)$ is defined as

$$a\Big(\boldsymbol{x},\frac{\boldsymbol{x}}{\varepsilon}\Big) = \frac{1.5+\sin(2\pi x/\varepsilon)}{1.5+\sin(2\pi y/\varepsilon)} + \frac{1.5+\sin(2\pi y/\varepsilon)}{1.5+\cos(2\pi x/\varepsilon)} + \sin(4x^2y^2) + 1, \tag{3.2}$$

with $\boldsymbol{x} = (x, y)$.

The domain D is a unit square $[0,1]\times[0,1]$. We first triangulate D into $NX\times NX$ small squares and then divide each square into two sub-triangles along its diagonal with positive ratio. As a start point, we test the accuracy of HMM, in particular, we consider the influence of microcell size over the accuracy. The results for the relative errors

$$\frac{\Big(\sum_{K\in\mathcal{T}_H}\|u^\varepsilon - \overline{u}^\varepsilon\|^2_{H^1(K)}\Big)^{1/2}}{\|u^\varepsilon\|_{H^1}}, \qquad \frac{\|u^\varepsilon - U_H\|_{L^2}}{\|u^\varepsilon\|_{L^2}} \qquad \text{and} \qquad \frac{\|u^\varepsilon - U_H\|_{L^\infty}}{\|u^\varepsilon\|_{L^\infty}}$$

are shown in Table 1, and plotted in Figure 3. The exact solutions u^ε are obtained by applying the Richardson extrapolation to the solutions by solving the problem with linear finite element on 1024×1024 and 2048×2048 meshes.

3.2.1. *Accuracy of HMM for two-scale problem.* We first fix the microcell size as $\delta = 1/32$, which is not an integer multiple of $\varepsilon = 1/79$.

NX	HMM		
	H^1 error	L^2 error	L^∞ error
8	0.4136e+00	0.1721e-01	0.1855e-01
16	0.2693e+00	0.1164e-01	0.1324e-01
32	0.7341e-01	0.6440e-02	0.7091e-02
64	0.3371e-01	0.8692e-02	0.1852e-01

TABLE 1. HMM for problem 3.1 with coefficient (3.2), $\varepsilon = 1/79$

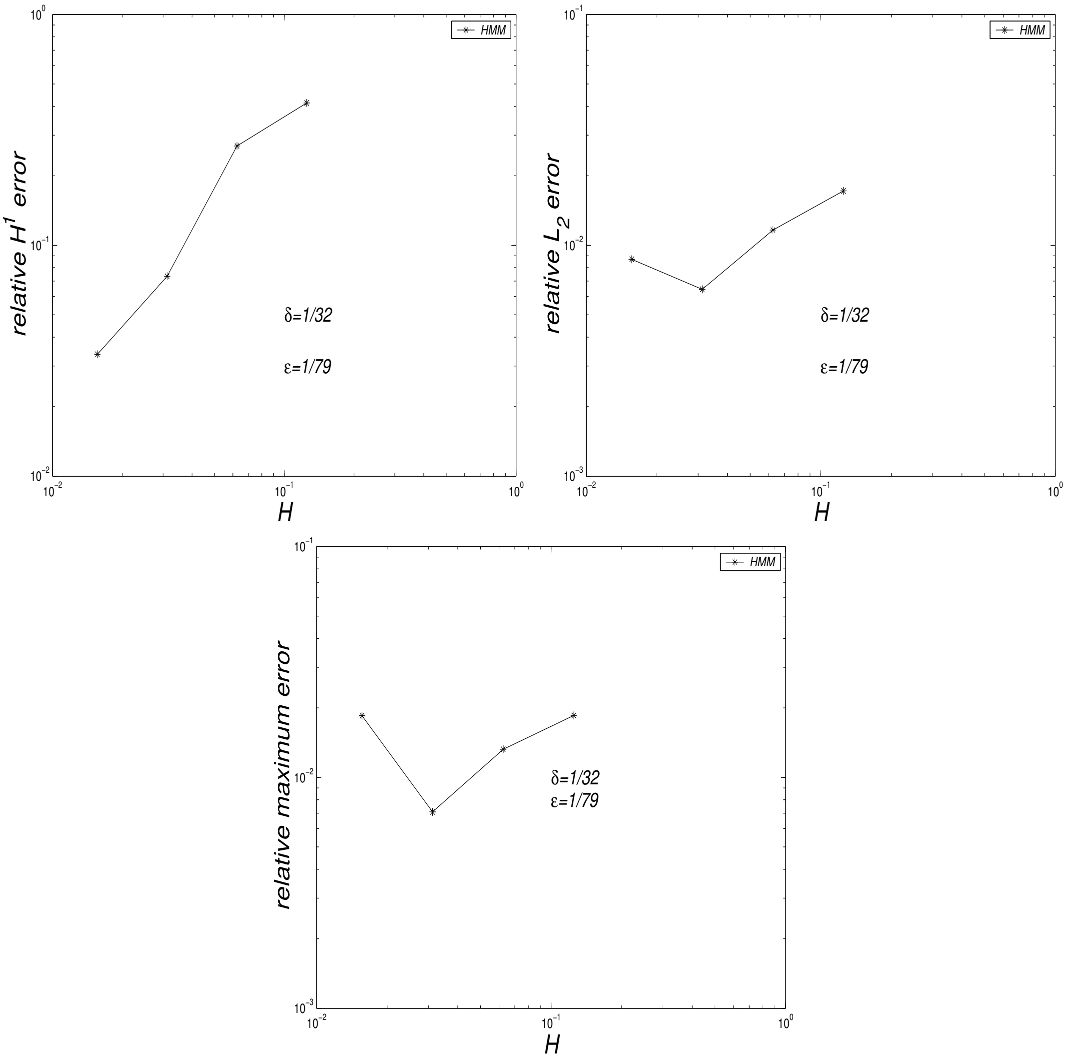

FIGURE 3. Relative error in H^1, L^2 and L^∞ norms of HMM for (3.1) with coefficients (3.2), where $\varepsilon = 1/79$

Notice that the error in H^1 norm is consistent with the previous theoretic result, e.g. Theorem 2.1, (2.12) and (2.13). However, in L^2 and L^∞ norms, the error increase at the finest mesh $H = 1/64$, instead of decrease as predicted by the error analysis. This scenario is not yet fully understood. But it should be due to the fact that in this case, the microcell is larger than the element, and some spurious information is sampled and polluted the HMM solution. This is hidden in the term $\mathcal{O}(\delta)$, which obviously has more chance to dominant the error in L^2 and L^∞ norms than that in H^1 norm.

Next we fix the mesh size as $H = 1/32$, and change the microcell size δ.

$1/\delta$	HMM		
	H^1 error	L^2 error	L^∞ error
16	0.5984e-01	0.8517e-02	0.1349e-01
32	0.7341e-01	0.6440e-02	0.7091e-02
64	0.1902e+00	0.6918e-02	0.7496e-01

TABLE 2. HMM for 3.1 with coefficient (3.2), $\varepsilon = 1/79$

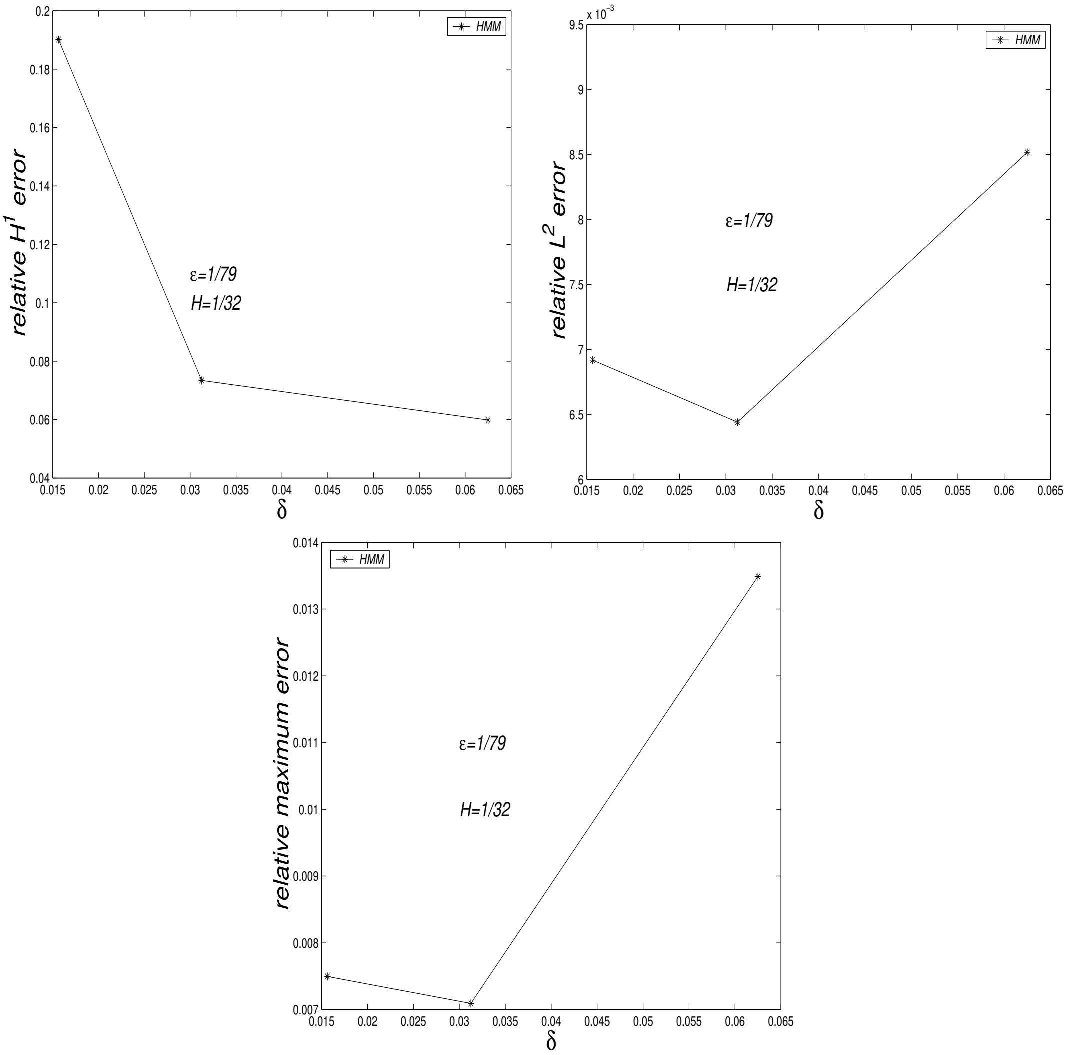

FIGURE 4. Relative error in H^1, L^2 and L^∞ norms of HMM for problem (3.1) with coefficients (3.2), where $\varepsilon = 1/79$

The results in Table 1, Table 2, Figure 3 and Figure 4 fit quite well with the theoretic results. Note that the error increase while the microcell is larger than the element.

3.2.2. *Comparison of HMM and MsFEM for two-scale problem.* In the following examples, we compare the convergence behavior for HMM and MsFEM. We first consider the case when δ is not an integer multiply of ε in HMM. We include the results for $\delta = H$. The size of the overlap for MsFEM is taken as $r = \varepsilon$ (see Figure 2).

NX	MsFEM			HMM		
	H^1 error	L^2 error	L^∞ error	H^1 error	L^2 error	L^∞ error
8	0.2423e+00	0.6393e-01	0.8425e-01	0.3023e+00	0.2250e-01	0.2326e-01
16	0.1272e+00	0.2388e-01	0.3607e-01	0.1181e+00	0.7764e-02	0.8997e-02
32	0.6682e-01	0.1102e-01	0.1948e-02	0.6292e-01	0.4694e-02	0.6038e-02
64	0.3950e-01	0.8291e-02	0.1533e-02	0.3598e-01	0.3930e-02	0.5247e-02

TABLE 3. HMM and MsFEM for 3.1 with coefficient (3.2), where $\varepsilon = 1/60$

Next, we consider a special case when $I_\delta = I_\varepsilon$ for HMM. The size of overlap for MsFEM is still $r = \varepsilon$. In this case, MsFEM can be modified to explicitly take into account the periodic structure of the original problem [28] by using the solutions of the cell problem as the basis function. But we will not consider this modification here, since the details are not yet published. The numerics are included in Table 4 and plotted in Figure 6.

NX	MsFEM			HMM		
	H^1 error	L^2 error	L^∞ error	H^1 error	L^2 error	L^∞ error
8	0.2445e+00	0.2831e-01	0.3201e-01	0.2459e+00	0.2094e-01	0.2179e-01
16	0.1276e+00	0.1278e-01	0.1460e-01	0.1258e+00	0.7894e-02	0.8467e-02
32	0.6902e-01	0.8533e-02	0.9745e-02	0.6434e-01	0.5138e-02	0.5553e-02
64	0.4246e-01	0.6815e-02	0.7818e-02	0.3462e-01	0.4202e-02	0.4599e-02

TABLE 4. HMM and MsFEM for (3.1) with coefficient (3.2), where $\varepsilon = 1/64$. I_ε is used as the microcell of HMM

In this case, both HMM and MsFEM give quite good results in H^1,L^2 and L^∞ norms. This is consistent with the error estimates in Theorem 2.1, Theorem 2.2 and Theorem 2.3.

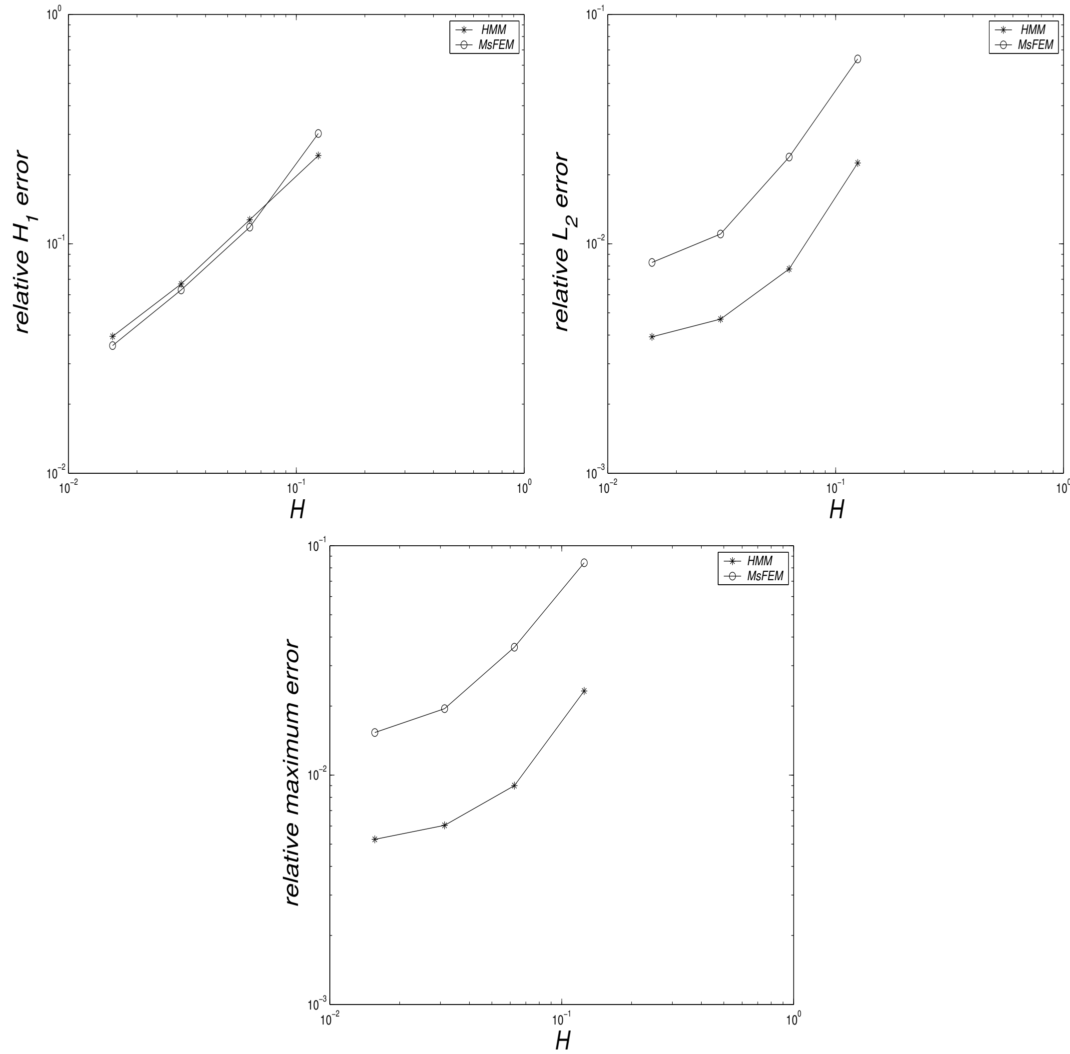

FIGURE 5. Relative error in H^1, L^2 and L^∞ norms for HMM and MsFEM for (3.1) with coefficient (3.2), where $\varepsilon = 1/60$ and $I_\delta = I_H$

Next we consider the case when the coefficient is random. Some care is required in this case. First of all, to have a well-defined exact solution to the fine scale problem, we will take the fine scale problem to be a finite difference analog of (1.1) on a 1024×1024 grid. The coefficients at the grid points are independent and have log-normal distribution with expectation $\mathbb{E} = 0$ and variance $\sigma^2 = 1$. Therefore effectively we have $\varepsilon = 1/1024$ [16]. For the HMM solution we choose δ to be H, and $r = H$ for MsFEM solution.

The leading order behavior in this case is determined by the solution of the homogenized equation, which is deterministic. The microscale information comes in at the next order, which is only reflected if one looks at the error in H^1 norm. The results in Figure 7, which are errors measured in L^2 and L^∞ norms respectively,

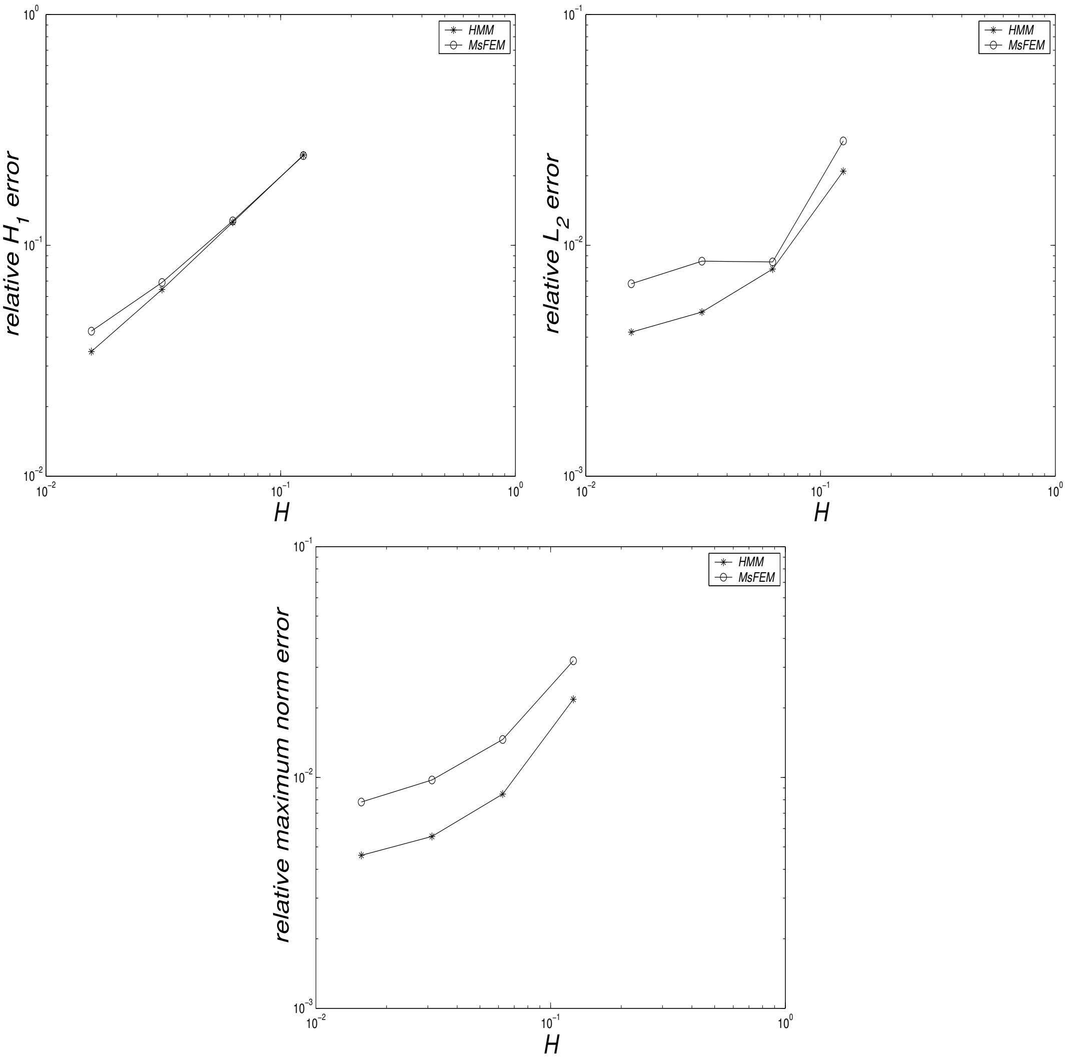

FIGURE 6. Relative error in H^1, L^2 and L^∞ norms for HMM and MsFEM for the two scale (3.1) with coefficient (3.2), where $\varepsilon = 1/64$. $I_\delta = I_\varepsilon$

suggest that both HMM and MsFEM captures the leading order behavior of the solution with reasonable accuracy. MsFEM has better accuracy when the macro-grid is very coarse. But HMM is more accurate upon refining the macroscale mesh. More importantly HMM displays a consistent rate of convergence as the coarse grid is refined. The accuracy of HMM on very coarse macro-grid can be improved by going to higher order HMM, as is discussed earlier in Section 2.

Next we discuss the issue of extracting the microscale information. This is important for many practical problems such as the stress distribution in a composite material and velocity field in a porous medium. From homogenization theory we know that the microscale information depends sensitively on the full details of the coefficients. Since in HMM the fine scale problem is only solved locally, one

NX	MsFEM			
	H^1 error(1)	H^1 error(2)	L^2 error	L^∞ error
8	0.2819e-01	0.2244e+00	0.1591e-01	0.1677e-01
16	0.1131e-01	0.1202e+00	0.9915e-02	0.1482e-01
32	0.8625e-02	0.8125e-01	0.9738e-02	0.1898e-01
64	0.8778e-02	0.9948e-01	0.1052e-01	0.2029e-01

TABLE 5. MsFEM for problem (3.1) with random coefficients, H^1 error (1) means the results are obtained with correction, and H^1 error (2) means the results are obtained without correction

NX	HMM			
	H^1 error(1)	H^1 error(2)	L^2 error	L^∞ error
8	0.3401e-01	0.2715e+00	0.3862e-01	0.3661e-01
16	0.1947e-01	0.2254e+00	0.2445e-01	0.2418e-01
32	0.4828e-02	0.2092e+00	0.7118e-02	0.9499e-02
64	0.4078e-02	0.2579e+00	0.6330e-02	0.9510e-02

TABLE 6. HMM for problem (3.1) with random coefficients, H^1 error (1) means the results are obtained with correction, and H^1 error (2) means the results are obtained without correction

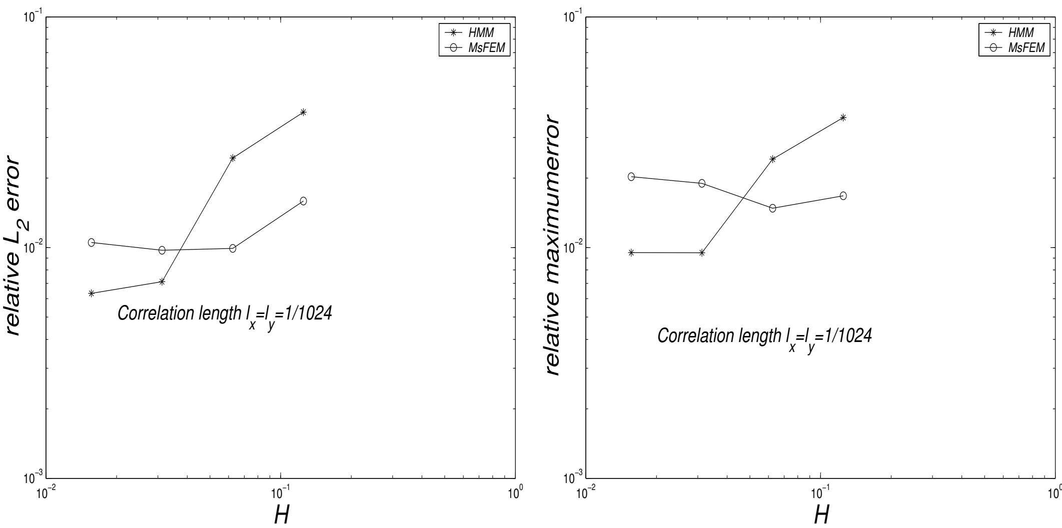

FIGURE 7. Relative error in L^2 and L^∞ norms for (3.1) with random coefficients.

cannot hope to recover accurately the details of the fine scale oscillations for each realization of the random field a^ε. Even though MsFEM does make use of the complete information on a^ε and does incur a cost that is at least comparable to that of solving the fine scale problem, the accuracy of MsFEM in H^1 norm (more precisely the piecewise H^1 norm in order to avoid the trouble caused by the discontinuity at the edges between elements), is not much better than 10%. In fact, to recover the fine scale oscillations accurately, one needs to solve the full fine scale problem. Therefore one should ask instead how the microscale information can be recovered locally, giving the leading order behavior. This is done using the local correction procedure discussed earlier. The results for both HMM and MsFEM are summarized in Table 5, Table 6 and Figure 8. Here we take K an arbitrarily chosen element and $\eta = 1/8$.

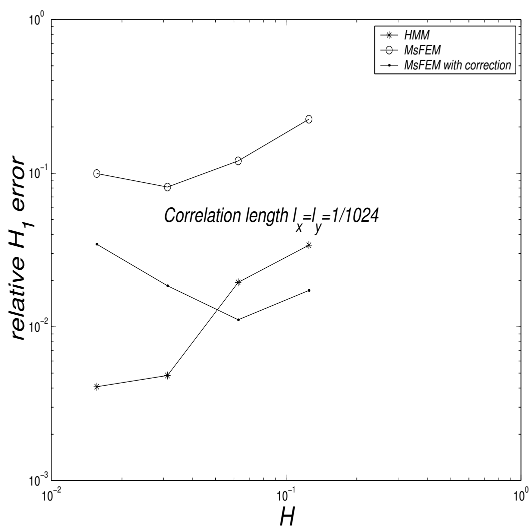

FIGURE 8. Relative error in H^1 norm for (3.1) with random coefficients

In view of these results, we see consistently that HMM is more accurate than MsFEM on finer macroscale mesh, but less accurate than MsFEM on coarser macroscale mesh. This is likely due to the fact that if the macroscale mesh is very coarse, HMM does not sample a^ε adequately since it only sample a small cell.

3.3. **MsFEM does not converge if the fine scale information is not explicitly used.** In what follows, we will show by an explicit example that MsFEM does not converge if the small scale information is not explicitly taken into account. Our strategy is similar to *finite difference homogenization* [33, 39].

Let $a^\varepsilon(\boldsymbol{x}) = k^\varepsilon(\boldsymbol{x})I$, where $k^\varepsilon(\boldsymbol{x})$ takes the values α and β as in Figure 9, ε is the size of the cell. We may write the coefficient matrix in the form as

$a^\varepsilon(\boldsymbol{x}) = a(x_1/\varepsilon, x_2/\varepsilon)$ with

$$a(y_1, y_2) = \begin{cases} \beta & 0 \le y_1 \le 1, 0 \le y_2 \le y_1, \\ \alpha & 0 \le y_1 \le 1, y_1 \le y_2 \le 1. \end{cases} \tag{3.3}$$

Without using explicitly the information about the size of the microscale, one may take $H = \varepsilon$. We will show in this case that the 'resonance error' remains finite even with oversampling as $H \to 0$. We will take the size of the overlap to be $\delta = rH$ with r fixed.

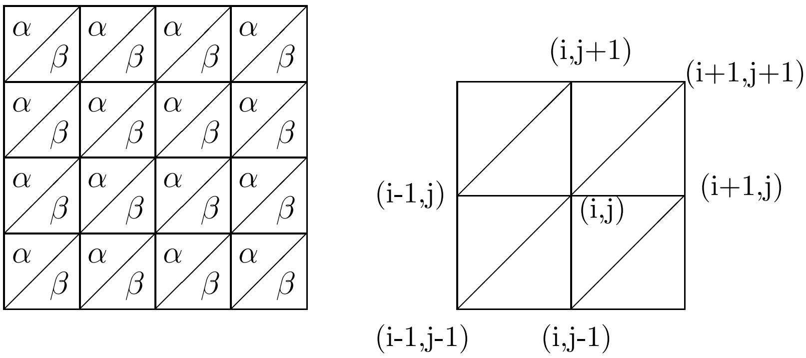

FIGURE 9. Left: Pattern for $\varepsilon = H$ Right: Element stiffness matrix

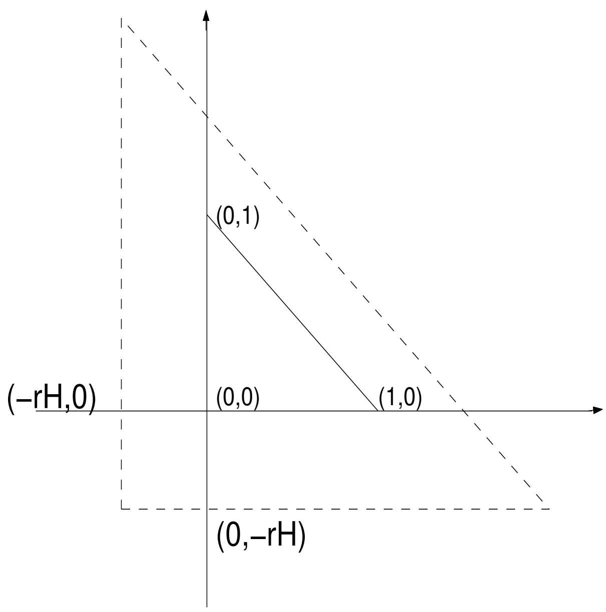

FIGURE 10. Pattern for $\varepsilon = H$ with overlap r

Lemma 3.1. *Except for the elements near the boundary, the stiffness matrix* $A = (A_{ij,k\ell})$ *in MsFEM with overlap has the structure:*

$$\begin{array}{llllll} A_{ij;i,j} &= b, & A_{ij;i-1,j} &= c, & A_{ij;i,j-1} = c, \\ A_{ij;i+1,j} &= c, & A_{ij;i,j+1} &= c, & \\ A_{ij;i-1,j+1} &= d, & A_{ij;i+1,j-1} &= d, & \end{array}$$

where b, c *and* d *depend on* r *but are independent of* H*. Moreover,*

$$b + 4c + 2d = 0. \tag{3.4}$$

Proof. This follows from the simple observation that after some reflection and translation if necessary, every element can be mapped by a simple scaling $(x, y) \to (x/H, y/H)$ to the standard element shown in Figure 10. We postpone the proof of (3.4) to the Appendix. □

Lemma 3.2. *As* $H \to 0$*, the solution of MsFEM converges to the solution of*

$$-e(r)\triangle U_0(\boldsymbol{x}) - 2f(r)\, U_{0,xy}(\boldsymbol{x}) = f(\boldsymbol{x}), \tag{3.5}$$

where $e(r) = -c - d$ *and* $f(r) = d$*.*

Proof. This follows directly from Lemma 3.1 by Taylor expansion. □

Lemma 3.3. *In the special case when* $r = 0$ *(no overlapping), then*

$$b = 2(\alpha + \beta), \qquad c = -\frac{\alpha + \beta}{2}, \qquad d = 0.$$

Proof. This is straightforward. □

As $\varepsilon = H \to 0$, the original problem, however, is a homogenization problem [7, 43], whose homogenized coefficient has the following property.

Lemma 3.4. *The homogenized coefficient matrix* A *has the following structure*

$$A = \begin{pmatrix} e^* & f^* \\ f^* & e^* \end{pmatrix},$$

where e^* *and* f^* *satisfy the following relation*

$$(e^*)^2 - (f^*)^2 = \alpha\beta. \tag{3.6}$$

To prove the above lemma, we first give a description for the properties of the homogenized coefficient matrix for the elliptic problem (1.1), which is denoted by A and is given by

$$A_{ij} = \int_0^1 \int_0^1 \Big(a_{kl} \frac{\partial \chi^i}{\partial x_k} \frac{\partial \chi^j}{\partial x_l} \Big)(\boldsymbol{x})\, d\boldsymbol{x}, \quad i, j = 1, 2,$$

where $\chi^j = x_j + N^j$, and N^j is periodic function that satisfies

$$-\frac{\partial}{\partial x_i}\Big(a_{ik} \frac{\partial N^j}{\partial x_k} \Big) = \frac{\partial a_{ij}}{\partial x_i}, \quad j = 1, 2. \tag{3.7}$$

Since a^ε is diagonal, we get

$$A_{ij} = \int_0^1 \int_0^1 \Big(a^\varepsilon \nabla\chi^i \nabla\chi^j\Big)(\boldsymbol{x})\, d\boldsymbol{x}. \tag{3.8}$$

Denote by $\bar{a}^\varepsilon$ and $\hat{a}^\varepsilon$ the coefficients obtained by reflecting the pattern in Figure 9 along the x_1 and x_2 axis, respectively (see Figure 11 below), $\bar{A}$ and $\hat{A}$ denote the corresponding effective coefficient matrix.

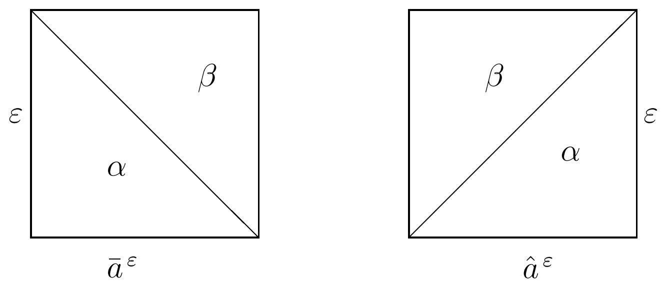

FIGURE 11. The pattern for the coefficients $\bar{a}^\varepsilon$ and $\hat{a}^\varepsilon$

Lemma 3.5. *If*

$$A = \begin{pmatrix} a & b \\ b & c \end{pmatrix},$$

then we have

$$\bar{A} = \begin{pmatrix} a & -b \\ -b & c \end{pmatrix}, \qquad \hat{A} = \begin{pmatrix} a & b \\ b & c \end{pmatrix}.$$

Proof. Denote by $\bar{N}^j$ the solutions of the cell problem (3.7) with coefficients $\bar{a}^\varepsilon$, then

$$\bar{N}^1(x,y) = N^1(x, 1-y) \qquad \bar{N}^2(x,y) = -N^2(x, 1-y). \tag{3.9}$$

In view of (3.8), we get the above expression for $\bar{A}$.

Proceeding in the same fashion, we get the above expression for $\hat{A}$. □

Proof for Lemma 3.4. Observe that A is symmetric since a^ε is symmetric, we thus assume

$$A = \begin{pmatrix} e^* & f^* \\ f^* & \tilde{e}^* \end{pmatrix}.$$

Since $\bar{a}^\varepsilon$ is symmetric with respect to the line $x = y$, we may conclude that

$$\bar{N}^1(x,y) = \bar{N}^2(y,x),$$

which implies $e^* = \tilde{e}^*$. Invoking Lemma 3.5, we have $A = \hat{A}$. Using the general duality principle in homogenization theory [44, Theorem 15.1] (see also [32]), we have

$$\mathcal{R} A \mathcal{R}^T \hat{A} = \operatorname{diag}(\alpha\beta, \alpha\beta),$$

where $\mathcal{R}$ is the rotation matrix with angle $\pi/2$ and $\mathcal{R}^T$ is the transpose matrix, i.e.,

$$\mathcal{R} = \begin{pmatrix} 0 & 1 \\ -1 & 0 \end{pmatrix}$$

From this we obtain $(e^*)^2 - (f^*)^2 = \alpha\beta$. $\square$

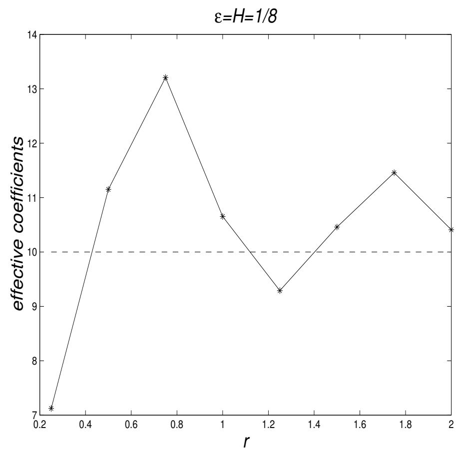

FIGURE 12. Comparison of $e^*(r)^2 - f^*(r)^2$ computed by MsFEM (the solid line) and the exact value of $(e^*)^2 - (f^*)^2 = 10$ (the dashed line)

We can check by direct computation whether (3.6) is satisfied by the solutions of MsFEM. When $r = 0$, we have $e(0) = \frac{\alpha+\beta}{2}$ and $f(0) = 0$, hence

$$e(0)^2 - f(0)^2 = \Big(\frac{\alpha+\beta}{2}\Big)^2 \neq \alpha\beta.$$

In Figure 12, we plot $e^*(r)^2 - f^*(r)^2$ as a function of r in case of $\alpha = 10$ and $\beta = 1$ hence $\alpha\beta = 10$. We can see that when $r > 0$, the error $e^*(r)^2 - f^*(r)^2 - \alpha\beta$ is reduced but stays finite, proving that there is a finite error in the solutions of MsFEM when $H \to 0$.

These findings are consistent with the error estimates in Theorem 2.3 suggesting that the term ε/H does play a role in the error.

To recover convergence to the correct solution within the framework of MsFEM, we need to take $H \gg \varepsilon$. However in this case as we indicated earlier, either MsFEM has to be modified to tailor to the specific periodic structure, or efficiency has to be greatly compromised.

4. Problems without scale separation

4.1. **Problems with many scales.** It has been observed that for some problems without scale separation, MsFEM does seem to give answers with reasonable accuracy. We have experimented with a number of such examples. We found that this is not special to MsFEM. HMM also shows the same tendency. In this case since there is no scale separation, we choose size of the cell I_δ to be the same as H. Hence there is no savings compared with the fine scale solver.

We show the result of one example with six scales. We solve (2.1) with the following coefficients.

$$
\begin{aligned}
a^{\varepsilon}(\boldsymbol{x}) = \frac{1}{6}\Big(& \frac{1.1+\sin(2\pi x/\varepsilon_1)}{1.1+\sin(2\pi y/\varepsilon_1)} + \frac{1.1+\sin(2\pi y/\varepsilon_2)}{1.1+\cos(2\pi x/\varepsilon_2)} + \frac{1.1+\cos(2\pi x/\varepsilon_3)}{1.1+\sin(2\pi y/\varepsilon_3)} \\
& + \frac{1.1+\sin(2\pi y/\varepsilon_4)}{1.1+\cos(2\pi x/\varepsilon_4)} + \frac{1.1+\cos(2\pi x/\varepsilon_5)}{1.1+\sin(2\pi y/\varepsilon_5)} + \sin(4x^2y^2)+1\Big),
\end{aligned}
\tag{4.1}
$$

where $\varepsilon_1 = 1/5, \varepsilon_2 = 1/13, \varepsilon_3 = 1/17, \varepsilon_4 = 1/31$ and $\varepsilon_5 = 1/65$. The right-hand side is $f = 10$. The coefficient at $y = 0$ is plotted in Figure 13.

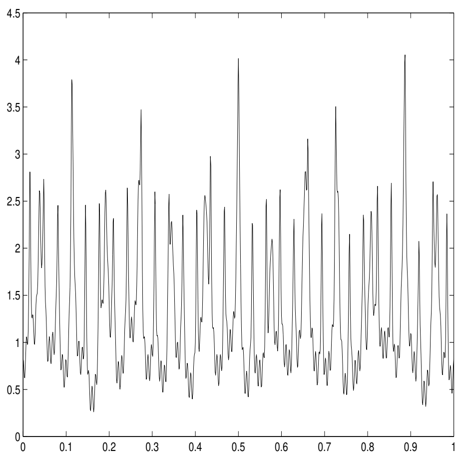

FIGURE 13. The coefficient (4.1) at $y = 0$

The results for the relative error in H^1, L^2 and L^∞ norms are plotted in Figures 14. As before the exact solution is obtained by extrapolating the numerical solutions on the 1024×1024 and 2048×2048 meshes. We can see from these results that the accuracy is substantially worse than the case with scale separation, but it is not catastrophic and maybe acceptable for some practical problems.

Even though the accuracy seems to be reasonable, one has to bear in mind two facts. The first is that in this case the cost of either HMM or MsFEM is no less than that of the fine scale solver. The second is that the accuracy is substantially less than that of the fine scale solver. In fact the example discussed earlier in 3.3 shows that in general one has to expect a finite error to remain in the limit as $H \to 0$. These considerations remove any interest of pursuing the issue further.

Compared with the two-scale problem addressed before, the above convergence history for both methods indicates quite pessimistic convergence rate, in particular for the results in H^1 norm. The oscillation is also significant in both methods, which may due to the resonance error between the different scales.

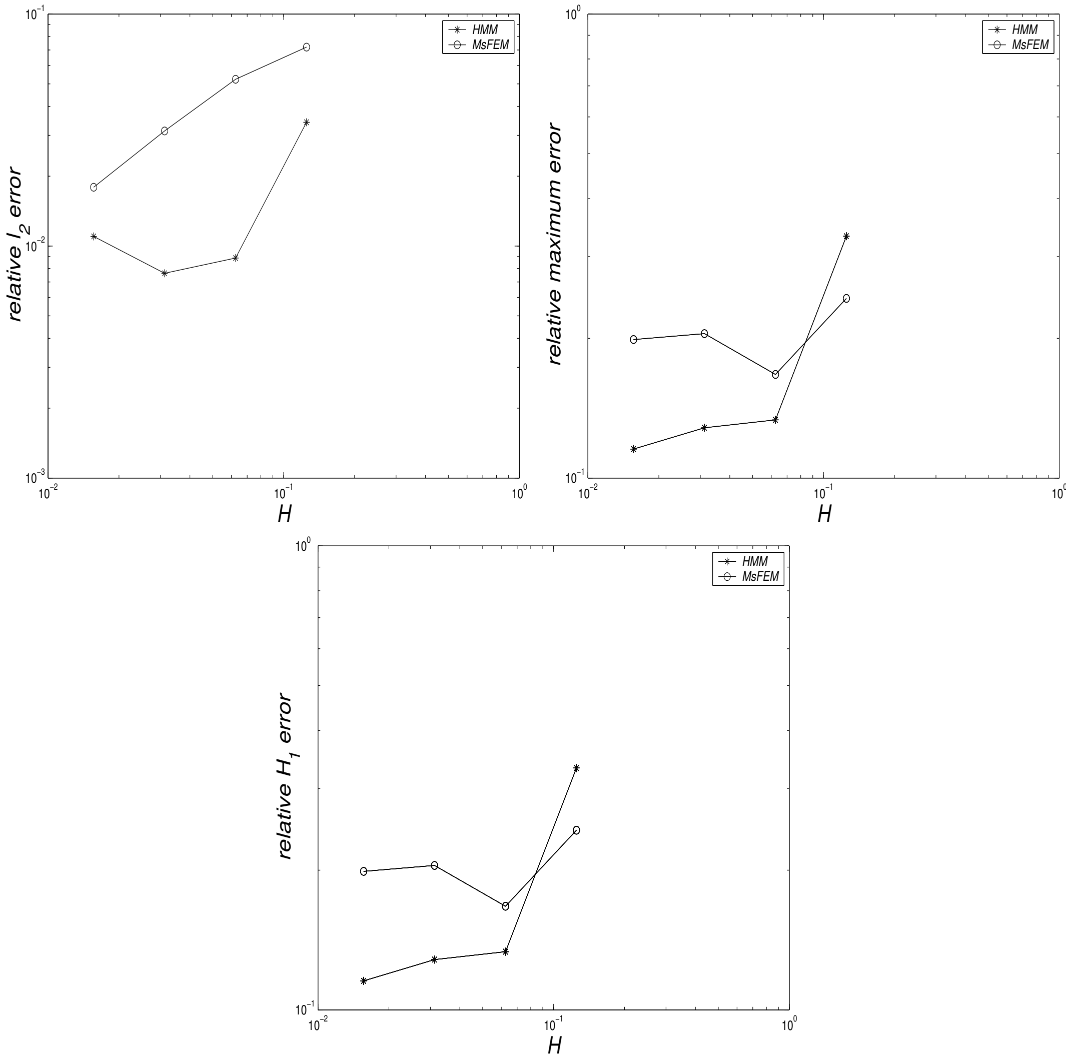

FIGURE 14. Relative error for HMM and MsFEM in H^1, L^2 and $\mathrm{L}^\infty-$norms for the problem (3.1) with coefficient (4.1)

4.2. **Problems with continuous spectrum.** Another often used example of problems without scale separation is the problem with random coefficients that have an algebraically decaying energy spectrum, i.e.,

$$\langle\, |\hat{a}(k)|^2 \,\rangle \simeq |k|^{-\alpha},$$

where $\langle\,\cdot\,\rangle$ denotes ensemble averaging, $\{\hat{a}(k)\}$ is the Fourier transform of the coefficients $a(x)$. Problems of this kind were used in [29] as examples without scale separation. We will demonstrate in this case that u has some degree of regularity depending on α, hence standard finite element methods converge with certain rate. Even there is no scale separation in this problems, the energy content decreases as the scale decreases. Hence there is relatively little energy at this small scale. This gives rise to the regularity of the solutions. Therefore, this class of problems are in fact much simpler than the one considered earlier in which the small scale and the large scale have the comparable amount of energy.

We consider the following problem:

$$\begin{cases} -\dfrac{d}{dx}\Big(a(x)\dfrac{du}{dx}\Big) = \dfrac{d}{dx}g(x) & \text{in } [0,1], \\ u(x) = 0 & x = 0, 1. \end{cases} \tag{4.2}$$

Here

$$a(x) = 1 + \frac{1}{2}\sin\Big(\sum_{k=1}^{\infty} k^{-\alpha}(\xi_{1k}\sin(kx) + \xi_{2k}\cos(kx))\Big), \tag{4.3}$$

with $\{\xi_{1k}\}$ and $\{\xi_{2k}\}$ are two independent random sequences uniformly distributed in $[-1/2, 1/2]$.

This problem by itself is specific, but our discussions are quite general. The regularity of $a(x)$ depends on the regularity of

$$g(x) = \sum_{k=1}^{\infty} k^{-\alpha}(\xi_{1k}\sin(kx) + \xi_{2k}\cos(kx)). \tag{4.4}$$

In particular for $\beta > 0$

$$\langle\, \|g(x)\|^2_{H^\beta} \,\rangle \le C \sum_{k=1}^{\infty} k^{2(\beta-\alpha)} < \infty,$$

if $\beta < \alpha - \frac{1}{2}$.

The exact solution satisfies

$$u_x(x) = \frac{g(x)}{1 + \frac{1}{2}\sin(g(x))}.$$

Hence we expect

$$\langle\, \|u(x)\|_{H^{1+\beta}} \,\rangle < \infty,$$

if $\beta < \alpha - \frac{1}{2}$. Consequently, the standard linear finite element method with mesh size h should have the estimate:

$$\langle\, \|u(x) - u_h(x)\|_{H^1} \,\rangle \le C h^\beta,$$

for β arbitrarily close to $\alpha - \frac{1}{2}$, if $0 < \alpha - \frac{1}{2} < 1$.

We performed numerical experiments on this problem. Plotted in Figure 15 and Figure 16 are the convergence history of the standard piecewise linear finite element method for one realization of (4.3) and (4.4) with $\alpha = 0.8$ and 1.2, respectively. We see that (4.3) is confirmed quite well.

To make a direct comparison between the different methods for this case would require tuning too many parameters. However this result and that of [29] do suggest that at the same cost the direct fine scale solver will perform at least as

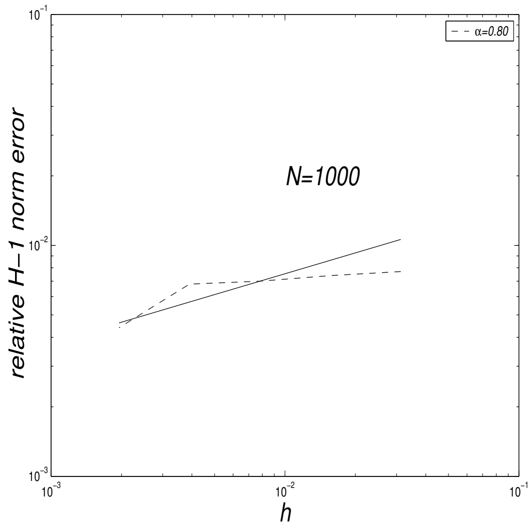

FIGURE 15. Relative H^1 error for $\alpha = 0.80$. The solid line is the reference curve for $h^{\alpha-1/2}$

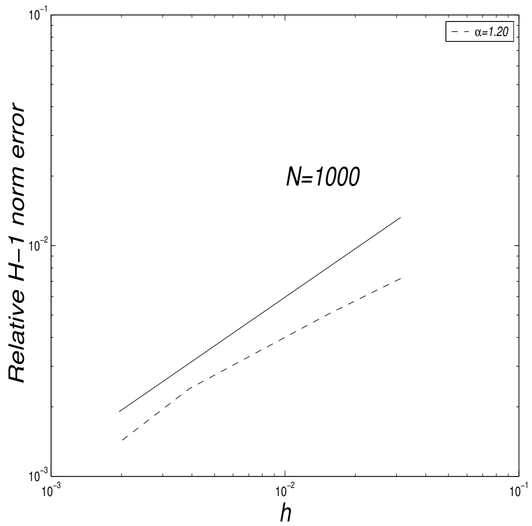

FIGURE 16. Relative H^1 error for $\alpha = 1.20$. The solid line is the reference curve for $h^{\alpha-1/2}$

well as MsFEM, because of the regularity of the exact solution. This is expected the same for HMM.

5. CONCLUSIONS

We have reviewed a variety of numerical techniques for solving the elliptic problem with multiscale coefficients. These techniques can be divided into two categories, those that are specifically designed for periodic homogenization problems and those that are applicable for more general problems. The former includes methods that solve the homogenized and corrector equations, finite elements methods that use multiscale test and trial functions. The latter includes HMM and MsFEM.

An important issue is how the cost of these methods compares with techniques such as multigrid for solving the full fine scale problem. In particular, whether some special features of the problems, such as scale separation, can be exploited to save cost. Nearly all the methods reviewed do have such savings for the special problem of periodic homogenization. For more general problems, the framework of HMM still allows us to take full advantage of any scale separation in the problem and therefore reduces the cost. This is different from MsFEM, which in general incurs a cost that is comparable to that of solving the full fine scale problem.

Many problems in practice do not have scale separation. Care has to be exercised when treating these problems. In the absence of any other special features of the problem, there is no hope to design numerical methods with sublinear cost compared with the fine scale solver. Therefore the task becomes identifying classes of problems with some other special features that can be made use of in order to reduce cost.

It has been suggested that MsFEM may have advantage compared with direct fine scale solver if the elliptic problem (1.1) is solved multiple times with different right-hand side. We note that other methods such as HMM and two-scale finite element method, have the same advantage. The potential savings that result from this remains to be carefully analyzed.

Appendix A. Proof of (3.4)

There are only two types of triangles in the pattern of Figure 9, i.e., we associate

Figure A.1

ϕ_i and ψ_i the MsFEM bases of i-th vertices in triangles K_1 and K_2, respectively. Define

$$\langle \phi_i, \phi_j \rangle = \int_{K_1} \nabla\phi_i \nabla\phi_j \, dx, \quad \langle \psi_i, \psi_j \rangle = \int_{K_2} \nabla\psi_i \nabla\psi_j \, dx.$$

Proof for (3.4) For ease of exposition, we drop the first subscript index of A. We first derive the following explicit expression for b, c and d.

$$b = 2\beta\langle \phi_2, \phi_2 \rangle + 2\alpha\langle \psi_3, \psi_3 \rangle - 2\beta\langle \phi_1, \phi_3 \rangle - 2\alpha\langle \psi_1, \psi_2 \rangle,$$

and

$$
\begin{aligned}
c &= -\frac{\beta}{2}\langle \phi_2, \phi_2\rangle - \frac{\alpha}{2}\langle \psi_3, \psi_3\rangle,\\
d &= \beta\langle \phi_1, \phi_3\rangle + \alpha\langle \psi_1, \psi_2\rangle.
\end{aligned}
$$

Due to the symmetry, we only consider a typical cell. Observed that

$$
\sum_{i=1}^{3} \phi_i = 1, \quad \sum_{i=1}^{3} \psi_i = 1,
$$

with

$$
\phi_1(x_1, x_2) = \phi_3(-x_2, -x_1), \quad \psi_1(x_1, x_2) = \psi_2(-x_2, -x_1). \tag{A.1}
$$

Obviously,

$$
b = \beta \sum_{i=1}^{3} \langle \phi_i, \phi_i\rangle + \alpha \sum_{i=1}^{3} \langle \psi_i, \psi_i\rangle.
$$

In view of the first observation, we get

$$
\begin{aligned}
&\Big(\langle \phi_1, \phi_1\rangle + \langle \phi_3, \phi_3\rangle - \langle \phi_2, \phi_2\rangle\Big) + 2\langle \phi_2, \phi_2\rangle\\
&= \Big(\langle \phi_1, \phi_1\rangle + \langle \phi_3, \phi_3\rangle - \langle \phi_1 + \phi_3, \phi_1 + \phi_3\rangle\Big) + 2\langle \phi_2, \phi_2\rangle\\
&= -2\langle \phi_1, \phi_3\rangle + 2\langle \phi_2, \phi_2\rangle.
\end{aligned}
$$

Similarly

$$
\sum_{i=1}^{3} \langle \psi_i, \psi_i\rangle = -2\langle \psi_1, \psi_2\rangle + 2\langle \psi_3, \psi_3\rangle.
$$

A combination of the above two leads to the expression for b.

It remains to prove the expression for c. We have $A_{i,j+1} = \beta\langle \phi_2, \phi_3\rangle + \alpha\langle \psi_1, \psi_3\rangle$ and $A_{i+1,j} = \beta\langle \phi_1, \phi_2\rangle + \alpha\langle \psi_2, \psi_3\rangle$. Due to observation (A.1), we get

$$
\begin{aligned}
\langle \phi_2, \phi_1 - \phi_3\rangle &= -\langle \phi_1 + \phi_3, \phi_1 - \phi_3\rangle\\
&= \langle \phi_3, \phi_3\rangle - \langle \phi_1, \phi_1\rangle\\
&= 0.
\end{aligned}
$$

Similarly, $\langle \psi_1, \psi_3\rangle = \langle \psi_2, \phi_3\rangle$. We thus have $A_{i,j+1} = A_{i+1,j}$, then

$$
2A_{i,j+1} = A_{i,j+1} + A_{i+1,j} = -\beta\langle \phi_2, \phi_2\rangle - \alpha\langle \psi_3, \psi_3\rangle,
$$

It follows the expression for c. The expression for d is obtained by the definition. With these expressions, it follows (3.4). $\square$

Acknowledgement. We thank Professor Weinan E and Professor Bjorn Engquist for inspiring discussions on the topic studied here.

References

1. R. A. Adams, *Sobolev Spaces*, Academic Press, 1975.
2. R. E. Alcouffe, A. Brandt, J. E. Dendy and J .W. Painter, *The multigrid method for the diffusion equation with strongly discontinuous coefficients*, SIAM J. Sci. Stat. Comput., **2**(1981), 430-454.
3. G. Allaire, *Homogenization and two-scale convergence*, SIAM J. Math. Anal., **23**(1992), 1482-1518.
4. I. Babuska, *Homogenization and its applications, mathematical and computational problems*, Numerical Solutions of Partial Differential Equations-III, (SYNSPADE 1975, College Park MD, May 1975), (B. Hubbard eds.), Academic Press, New York, 1976, 89-116.
5. I. Babuska, *Solution of interface by homogenization I, II, III*, SIAM J. Math. Anal., **7** (1976), pp. 603-634, pp. 635-645, **8** (1977), 923-937.
6. I. Babuska, G. Caloz and J. Osborn, *Special finite element methods for a class of second order elliptic problems with rough coefficients*, SIAM J. Numer. Anal., **31** (1994), 945-981.
7. I. Babuska and J. Osborn, *Generalized finite element methods: their performance and their relation to mixed methods*, SIAM J. Numer. Anal., **20** (1983), 510-536.
8. C. C. Battaile, D. J. Srolovitz, I. I. Oleinik, D. G. Pettifor, A. P. Sutton, S. J. Harris and J. E. Butler, *Etching effects during the chemical vapor deposition of (100) diamond*, J. Chem. Phys., **111**(1999), 4291-4299.
9. A. Benssousan, J. L. Lions and G. Papanicolaou, *Boundary layer analysis in homogenization of diffusion equations with Dirichlet cnditions on the half spaces*, Proceedings of International Symposium on Stochastic Diffenertial Equations (Kyoto) (K. Ito, eds.), Wiley, 1976, 21-40.
10. A. Benssousan, J. L. Lions and G. Papanicolaou, *Asymptotic Analysis of Periodic Structures*, North-Holland, 1978.
11. J. F. Bourgat, *Numerical experiments of the homogenization method for operators with periodic coefficients*, Lecture Notes in Mathematics, Vol 707. 330-356.
12. A. Brandt, *Multi-level adaptive solutions to boundary-value problems*, Math. Comp., **31** (1977), 333-390.
13. F. Brezzi, L. P. Franca, T. J. R. Hughes and A. Russo, $b = \int g\,dx$, Comput. Methods Appl. Mech. Engrg., **145** (1997), 329-339.
14. Z. Chen and T. Y. Hou, *A mixed multiscale finite element method for elliptic problems with oscillating coefficients*, Math. Comp., **72** (2003), 541-576.
15. P. G. Ciarlet, *The Finite Element Method for the Elliptic Problems*, North-Holland, Amsterdam, 1978.
16. J. G. Conlon and A. Naddaf, *On homogenization of elliptic equations with random coefficients*, Elec J. Prob., **5** (2000), 1-58.
17. J. Z. Cui and L. Q. Chao, *The two-scale analysis methods for woven composite materials*, Engineering Computation and Computer Simulation I, (Zhi-hua Zhong eds.), Hunan University Press, 1995, 203-212.
18. L. J. Durlofsky, *Numerical-calculation of equivalent grid block permeability tensors for heterogeous porous media*, Water Resour. Res., **27**(1991), 699-708.
19. M. Dorobantu and B. Engquist, *Wavelet-based numerical homogenization*, SIAM J. Numer. Anal., **35** (1998), pp. 540-559.
20. W. E, *Homogenization of linear and nonlinear transport equations*, Comm. Pure Appl. Math., **45**(1992), 301-326.
21. W. E and B. Engquist, *The heterogeneous multiscale methods*, Comm. Math. Sci., **1**(2002), 87-132.

22. W. E and B. Engquist, *The heterogeneous multiscale method for homogenization problems*, submitted to MMS, 2002.
23. W. E and B. Engquist, *Multiscale modeling and computation*, 2003, to appear in Notices of AMS.
24. W. E, P. Ming and P. Zhang, *Analysis of the heterogeneous multiscale method for elliptic homogenization problems*, preprint, 2002.
25. Y. R. Efendiev, T. Y. Hou and X. Wu, *Convergence of a nonconforming multiscale finite element method*, SIAM J. Numer. Anal., **37** (2000), 888-910.
26. B. Engquist and O. Runborg, *Wavelet-based numerical homogenization with applications*, Multiscale and Multiresolution Methods: Theory and Applications, Lecture Notes in Computational Sciences and Engineering, Vol 20, (T. J. Barth, T. Chan and R. Heimes ed.), Springer-Verlag, 2002, 97-148.
27. L. Greengard and V. Rokhlin, *A fast algorithm for particle simulations*, J. Comp. Phys., **73** (1987), 325-348.
28. T. Y. Hou, private communication, 2003.
29. T. Y. Hou and X. Wu, *A multiscale finite element method for elliptic problems in composite materials and porous media*, J. Comput. Phys., **134**(1997), 169-189.
30. T. Y. Hou, X. Wu and Z. Cai, *Convergence of a multiscale finite element method for elliptic problems with rapidly oscillation coefficients*, Math. Comp., **68**(1999), 913-943.
31. T. J. R. Hughes, *Multiscale phenomena: Green's functions, the Dirichlet to Neumann formulation, subgrid, scale models, bubbles and the origin of stabilized methods*, Comput. Methods Appl. Mech. Engrg., **127** (1995), 387-401.
32. J. B. Keller, *A theorem on the conductivity of a composite medium*, J. Math. Phys., **5** (1964), 548-549.
33. S. M. Kozlov, *Averaging of difference schemes*, Math. USSR Sbornik., **57** (1987), 351-369.
34. A. M. Matache, I. Babuska and C. Schwab, *Generalized p-FEM in homogenization*, Numer. Math., **86** (2000), 319-375.
35. A. M. Matache and C. Schwab, *Two-scale finite element for homogenization problems*, M2AN., **36** (2002), 537-572.
36. N. Neuss, W. Jäger and G. Wittum, *Homoginization and multigrid*, Computing., **66** (2001), 1-26.
37. G. Nguetseng, *A general convergence result for a functional related to the theory of homogenization*, SIAM J. Math. Anal., **20** (1989), 608-623.
38. J. T. Oden and K. S. Vemaganti, *Estimation of local modelling error and global-oriented adaptive modeling of heterogeneous materials: error estimates and adaptive algorithms*, J. Comput. Phys., **164** (2000), 22-47.
39. A. Piatnitski and E. Remy, *Homogenization of elliptic difference operators*, SIAM J. Math. Anal., **33** (2001), 53-83.
40. G. Sangalli, *Capturing small scales in elliptic problems using a Residual-Free Bubbles finite element method*, Multiscale Model. Simul., **1** (2003), 485-503.
41. C. Schwab, *Two-scale FEM for homogenization problems*, Mathematical Modeling and Numerical Simulation in Continuum Mechanics, (I. Babuska, P. G. Ciarlet and T. Miyoshi ed.), Lecture Notes in Computational Science and Engineering, Vol 19, Springer-Verlag 2002, 91-108.
42. C. Schwab and A.-M. Matache, *Generalzied FEM for homogenization problems*, Multiscale and Multiresolution Methods: Theory and Applications, Lecture Notes in Computational

Sciences and Engineering, Vol 20, (T. J. Barth, T. Chan and R. Heimes ed.), Springer-Verlag, 2002, 197-238.
43. L. Tartar, *Estimations de coefficients homogénéisés*, Lecture notes in Mathematics, Vol. 704, Springer-verlag, Berlin, 364-373.
44. S. Torquato, *Random Heterogeneous Materials: Microstructure and Macroscopic Properties*, Springer-Verlag, New York, 2002.
45. X.-Y. Yue, *Numerical homogenization for well-driven transport in heterogeneus media*, Report, Institute of Computational Mathematics, AMSS, Chinese Academy of Sciences, 2002.
46. V. V. Zhikov, S. M. Kozlov and O. A. Oleinik, *Homogenization of Differential Operators and Integral Functionals*, Springer-verlag Berlin Heidelberg, 1994.

A1 South 4 Street, Zhong Guan Cun, Institute of Computational Mathematics, Academy of Mathematics and System Sciences, Chinese Academy of Sciences, Bei Jing 100080, China
E-mail address: mpb@lsec.cc.ac.cn
Current address: PACM, Department of Mathematics, Princeton University, NJ 08544, USA

Department of Mathematics, Suzhou University, Suzhou, 215006 China
E-mail address: xyyue@suda.edu.cn